

How to design, develop and build a fully-integrated melt electrowriting 3D printer



Kian F. Eichholz^{a,b,c,*}, Inês Gonçalves^{a,b,c}, Xavier Barceló^{a,b,c}, Angelica S. Federici^{a,b,c}, David A. Hoey^{a,b,c}, Daniel J. Kelly^{a,b,c,d}

^a Trinity Centre for Biomedical Engineering, Trinity Biomedical Sciences Institute, Trinity College Dublin, Ireland

^b Department of Mechanical, Manufacturing and Biomedical Engineering, School of Engineering, Trinity College Dublin, Ireland

^c Advanced Materials and Bioengineering Research Centre (AMBER), Royal College of Surgeons in Ireland and Trinity College Dublin, Ireland

^d Department of Anatomy, Royal College of Surgeons in Ireland, Dublin, Ireland

ARTICLE INFO

Keywords:

MEW
Melt electrowriting
Hardware
Design and build
Custom

ABSTRACT

Melt electrowriting (MEW) is a high resolution material extrusion based additive manufacturing process with the unique capability to produce micron to sub-micron diameter fibres and control their deposition in three dimensions. Here, we detail the design, development and build of a custom MEW printer which has full integration between all core components. We detail the design and build of the motion system, print head (including heaters, extrusion system and high voltage power supply) and safety systems, and explain how these are integrated via a central control unit to provide pre-programmed dynamic control over printing variables allowing the fabrication of a range of advanced material designs with applications in the fields of tissue engineering, regenerative medicine and beyond. We discuss the various approaches which may be used for each system within a custom MEW printer, providing an insight into how it may be designed depending on the specific requirements of the end user. Finally, we demonstrate the capabilities of this printer by producing tissue engineering scaffolds with various architectures. This work aims to make MEW technology more accessible by both informing others interested in developing similar custom devices, and additionally, by providing an insight into the inner workings of MEW technology for practitioners in the field.

1. Introduction

Melt electrowriting (MEW) is a high resolution additive manufacturing process which utilises a high voltage between a print nozzle and collector to stabilise the flow of print material, allowing precise controlled deposition of micron to sub-micron diameter fibres. This technique was first demonstrated in 2011 [1,2] and has since gained substantial popularity and widespread use, in particular for the development of tissue engineered scaffolds [3,4]. Its use for tissue engineering applications is popular due to the high porosities and low fibre diameters achievable by MEW fabricated structures, enabling the fabrication of complex microarchitectures tailored to engineering specific biological tissues. In addition, the technique has demonstrated versatility for other industrial applications such as manufacturing embedded microchannel systems [5] and glass chips for applications such as optics, photonics and “lab-on-a-chip” devices [6].

While this technology is still in its relative infancy, MEW has

undergone rapid growth and development since its inception. Indeed, the pre-cursor in the development of MEW technology entailed the manual movement of an x-y collecting stage to control the deposition of fibres [7], while present day technology has progressed to the development of highly complex printers such as those with expansive automated systems [8] and machine vision tools [9] for real time altering and monitoring of process variables. There have been several other key milestones within this developmental history. It has been demonstrated that tubular scaffolds can be fabricated using MEW by printing on a rotating mandrel [10], with later work developing an open source software to further enhance ease of use [11]. The printing of fibres with sub-micron diameters has also been demonstrated, further expanding the design space within which scaffolds may be fabricated [12]. Key developments in MEW technology entailed the incorporation of in-process control of print parameters, namely voltage to allow the fabrication of large volume scaffolds exceeding 7 mm in height [13], and pressure to allow variable fibre diameters within a single scaffold and

* Corresponding author at: Trinity Centre for Biomedical Engineering, Trinity Biomedical Sciences Institute, Trinity College Dublin, Ireland.
E-mail address: eichholz@tcd.ie (K.F. Eichholz).

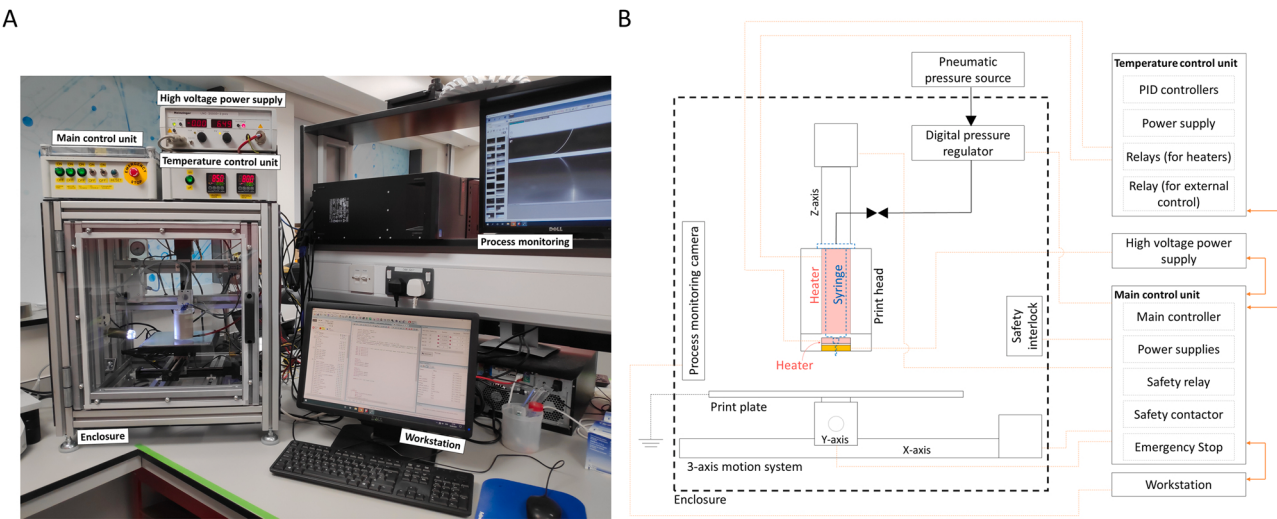


Fig. 1. **A** Photograph of one of the completed MEW 3D printers. **B** Control schematic for main components of the MEW printers. Please see “[Fig. 1.png](#)” in supplementary files for high resolution source image file of figure.

print job [14]. These latter developments require the use of complex printers with integrated motion, pressure (for material extrusion) and high voltage systems which can have variable pre-programmed outputs throughout the duration of the print job. Other key developments include the development of high throughout, multi-print head systems to scale up manufacturing [15], and the development of cell electro-writing technology to print cells within hydrogel microfibers [16].

There are several key components within a MEW printer, including the motion system to define fibre deposition, heating system to melt the print material for deposition, extrusion system to dispense the material through a nozzle/needle, high voltage system to stabilise the print jet, and safety systems due to the various hazards of MEW, in particular the high voltages involved. While several companies have recently developed and began to provide commercially available MEW printers, many researchers continue to use custom built systems. Firstly, due to the relative youth of the technology, researchers previously had no choice but to build custom MEW printers in absence of any commercially available units. In addition, building a custom MEW printer is more cost effective, provided that sufficient expertise and time are present to undertake this process. The greatest argument in favour of implementing a custom built MEW printer, however, lies in the flexibility to design a system specific to the requirements and complexities of the end user in question. Finally, it is worth noting that several commercially available MEW printers are in essence modified 3D printers with MEW print heads attached, which were initially designed for other additive manufacturing technologies. Such systems therefore lack some of the capabilities and features present in custom MEW printers which have been designed from the ground up with MEW printing in mind. End users should also be aware of the potential performance and reproducibility issues some of these systems have and perform due diligence if selecting a commercially available option.

When developing a custom MEW printing system, there are a range of possibilities available, from more simple and inexpensive systems which are relatively simple to implement [17], to complex fully automated systems with real-time process monitoring [18]. More simple designs consistent of discrete systems, for example, a separate high voltage power supply, pressure source or syringe pump, motion system and heating system, all of which are controlled manually and independently. Such a system can be implemented relatively quickly, for example, by utilising a commercial 3-axis computer numerical control (CNC) gantry, high voltage power supply, and components for a print head (including heater(s) and a pressure source). In any case, pneumatic pressure is recommended over a syringe pump or screw extruder as it

provides a much smoother flow profile which is crucial for forming a consistent polymer jet and minimising instabilities. The print head is perhaps the most difficult system to develop, as the polymer must be melted while simultaneously applying a high voltage between the nozzle and print substrate. Electrical interference and arcing between the high voltage supply and the heating system is a potential issue here. This can easily be overcome by using heated air [17,19] or water [1] for example, however, these methods can cause issues in terms of slight temperature fluctuations and jet instabilities, or limited melt temperatures achievable. Here, we recommend the use of resistive heating elements, which can be electrically isolated from the high voltage supply as outlined in our methods below. Alternatively, the high voltage can be applied to the print plate while the nozzle can be grounded, a strategy which has successfully been used by other researchers [20], in addition to commonly being used in commercial MEW printers. Finally, the level of component integration is important to consider, and at the very least, we recommend integration between the motion system and the high voltage system if scaffolds above a height of approximately 1–2 mm are required. This allows voltage to be incrementally changed throughout the print job, which is necessary for producing high quality large volume scaffolds [13]. Further integration of other components such as the pressure source will allow for the formation of more complex structures with variable fibre diameters. Integration of the heaters primarily aids in terms of ease of use, as they can be shut down automatically at the end of the print job. In the following work we focus primarily on the hardware and design challenges when developing a custom MEW printer, however, there are other challenges associated with using a MEW printer. Thus, we recommended the following excellent articles, including a video and written tutorial on using MEW printers [21], a review on some of the materials challenges faced when MEW printing and the many materials which have successfully been used for fabricating melt electrowritten structures [22], and some publications which discuss the history and future potential of MEW [3,4,23].

In this work, we detail the complete design and build of a custom MEW printing system, with two almost identical printers (one with a fixed collector and one with an easily removable collector which can be interchanged with a rotating mandrel) being built as outlined. These MEW printers feature advanced capabilities which are not present in the majority of commercially available systems, including the complete integration of all key components which gives the user outright control over processing parameters for the fabrication of a wide range of biomaterial scaffold designs. We detail the development of the framing, motion system, print head assembly (including control over print

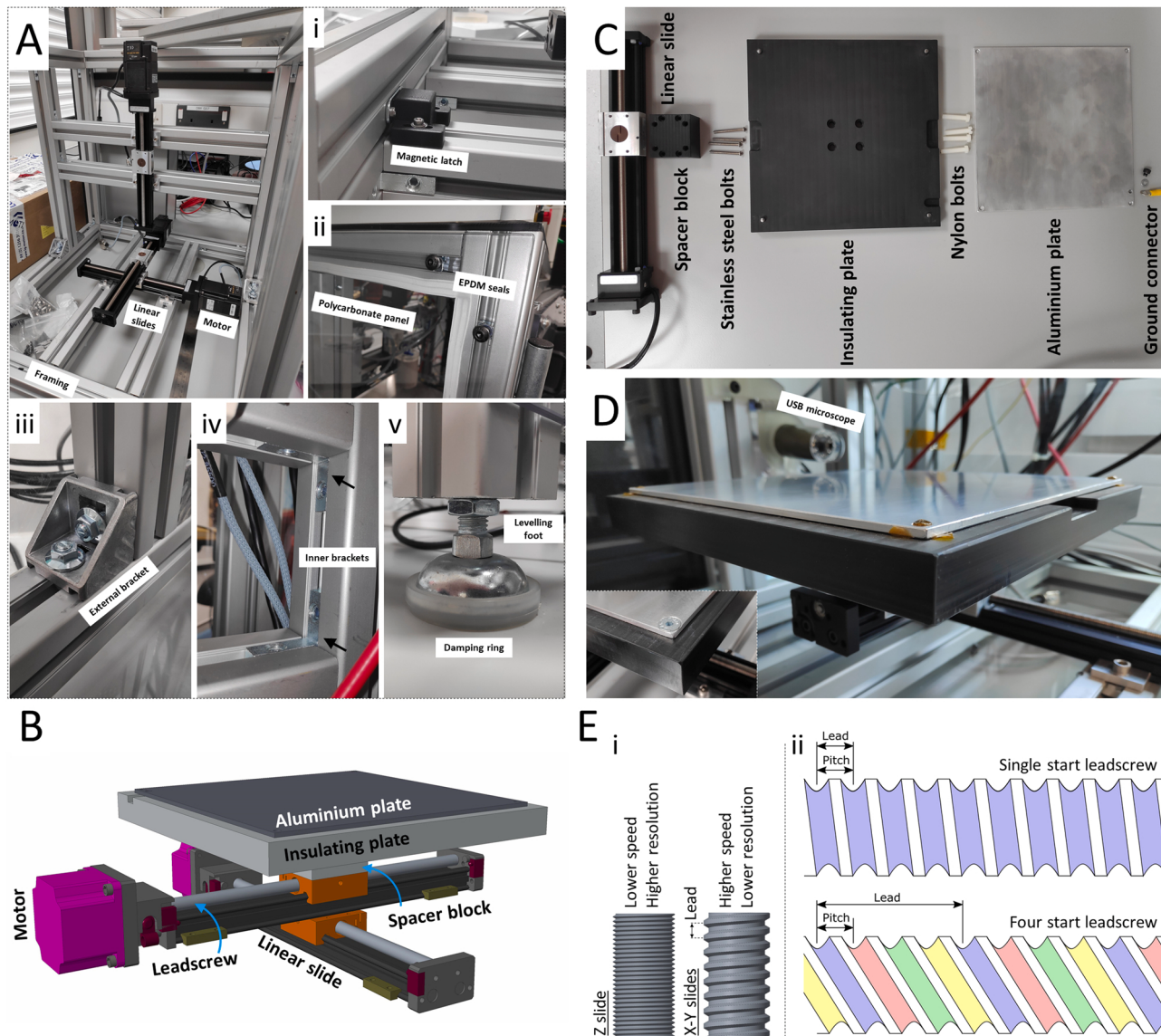


Fig. 2. Frame and motion system for MEW printer. **A** Frame construction and mounting of linear slides and motors. Illustrated are (i) the magnetic door latch, (ii) EPDM rubber sealed frame with polycarbonate panels attached, (iii) external angle brackets to support the printer gantry, (iv) inner brackets to assemble all other joints between aluminium profiling and (v) adjustable levelling feet with damping rings. **B** CAD design of X-Y stage and print plate assembly. **C** Exploded assembly view of print plate assembly. **D** Completed print plate assembly on frame with one configuration showing the plate mounted using dowel pins for quick removal, and the inset showing an alternative approach with the aluminium plate bolted to the insulating plate. **E** (i) Leadscrew characteristics for each linear slide and (ii) schematic demonstrating a single start leadscrew (used on the Z slide) and four start leadscrew (used on the X and Y slides). Please see “Fig. 2.png” in supplementary files for high resolution source image file of figure.

temperature, extrusion pressure and high voltage), a rotating mandrel for tubular scaffolds, and comprehensive information on the wiring and integration of all these components to a central control unit. We then demonstrate some of the key capabilities of these printers, including the ability to print large volume scaffolds with layer by layer voltage control, the printing of nanoscale fibres, hybrid printing capabilities combining both fused deposition modelling (FDM) and MEW additive manufacturing principles, variable fibre diameter scaffold fabrication via layer by layer extrusion pressure control and automated fibre stabilisation, printing of complex geometries via DXF (Drawing Exchange Format) files, and finally the printing of tubular MEW scaffolds. We also discuss numerous alternative configuration possibilities and varying levels of component integration depending on the requirements of the end user. This work aims to provide a comprehensive guide for anyone considering the implementation of a custom MEW printer, and additionally, to provide a detailed resource for those looking to learn more

about this fascinating and powerful additive manufacturing technology.

2. Materials and methods

2.1. Overview of custom MEW design

The MEW printer described here is comprised of a 4-axis motion system (3 main axes in XYZ directions and a 4th motion axis which may be used for a rotating mandrel), a print head assembly (comprised of heaters to control material temperature and a system for high voltage application), digital pressure controller, high voltage power supply and various safety systems. Two such MEW printers were built, with one being shown in Fig. 1A. All of the systems within the MEW printers are fully integrated and controlled through a central “main control unit”, as shown in the general control schematic in Fig. 1B. Custom parts were designed with PTC Creo Parametric 3.0 computer aided design (CAD)

software. Wiring diagrams were created with QElectroTech 0.80 software.

In the below Materials and methods sub-sections, we will outline each of the components within this custom designed MEW in greater detail. While all components are fully integrated in this system, it is important to note that this is not essential, and more simple configurations may be built according to the needs and cost requirements of the user. For example, in a previous study, the authors built a low-cost custom MEW with separate systems, with the exception of the high voltage power supply which was connected to a safety interlock [17]. Other examples and possible configurations will be discussed in greater detail in the Results and discussion section further below.

2.2. Framing and motion system

The chassis and frame was built using Bosch Rexroth 45 × 45 mm square aluminium profile. This provides a stable and rigid structure upon which other components can easily be mounted using the integrated attachment grooves. Fig. 2A illustrates the construction of the frame and various fittings. A magnetic latch was used to hold the door closed (Fig. 2A-i). Ethylene propylene diene monomer (EPDM) rubber strips were affixed to the exterior of the frame and polycarbonate panels of thickness 5 mm bolted on to ensure effective sealing (Fig. 2A-ii). External angle brackets were used to securely support the printer gantry (Fig. 2A-iii), while inner brackets were used in all other joints (Fig. 2A-iv). Adjustable levelling feet with damping rings were mounted underneath the frame (Fig. 2A-v).

The design concept for the print plate assembly is illustrated in Fig. 2B. This assembly consists of two motors and two linear slides (defining the XY motion of the printer), with a print plate mounted on top using either 4 pins or screws. Of note are the spacer block, which provides clearance for the print plate over the motor housing, and the insulating plate, which further isolates the aluminium plate from the linear slides and surrounding electrically conductive components in the chassis. This is achieved by the thickness of the insulating plate, and its larger outer dimensions of 230 × 230 mm (compared to the outer dimensions of 210 × 210 mm for the aluminium plate), giving a 10 mm insulating buffer region all around the aluminium plate. Nylon screws are further used to attach the insulating plate to the spacer block, as seen in the exploded assembly view in Fig. 2C. This design helps to completely isolate the grounded aluminium plate from all surrounding electrically conductive components, ensuring that a stable ground is defined upon which to perform MEW printing. This design allows an inverse configuration whereby the user may safely apply the high voltage to the print plate (and ground the nozzle) while avoiding electrical arcing to surrounding components. An image of the entire print plate assembly is shown in Fig. 2D, also illustrating the mounting of a USB microscope at the side of the frame for process visualisation and imaging of MEW fibres. In one of the MEW printers built, the aluminium plate is mounted using pins to allow quick removal of the plate for attachment of a rotating mandrel (Fig. 2D). In the second MEW printer, the print plate is mounted using countersunk bolts (Fig. 2D, inset).

It is important to consider the leadscrew pitch and lead for each axis in a MEW printer. The pitch is the distance between two adjacent threads, while the lead is the distance the carriage moves for one full rotation of the leadscrew (Fig. 2E). A high lead allows higher maximum linear speeds to be reached at the expense of resolution, while a lower lead results in a lower maximum speed but greater resolution (Fig. 2E-i). For the 2 slides defining XY motion, an intermediate to high lead is desirable, with a Velmex E02 leadscrew being chosen here, which has a lead of 0.2" (5.08 mm) and pitch of 1.27 mm. This is due to the fact that relatively high translation speeds are required to print straight fibres, particularly for lower fibre diameters. The XY slides have a four-start leadscrew design, meaning that there are four intertwined threads running parallel to one another, where the lead is 4 times the pitch (Fig. 2E-ii). This allows greater leads to be used without compromising

Table 1
Components for framing and motion system.

Component	Description/Material	Source	Part number
Framing	Aluminium Strut 45 × 45 mm	Radionics Ltd	493-8296
X and Y linear slides	Xslide 200 mm scan, 0.2" (5.08 mm) leadscrew	Velmex	XN-10-0080-E02-21
Z slide	Xslide 100 mm scan, 0.025" (0.635 mm) leadscrew	Velmex	XN10-0040-E25-21
Motors	Motor and drive - NEMA 23 2-stack AdvDrv 3 A, 500 micro 12–48 VDC	Arcus	ARCUS-DMX-A2-DRV-23
Motion system fittings	Various	Velmex	V-XMC-5 V-XMC-2
Framing fittings	Various (brackets, gussets, nuts, handle, feet, ring dampers)	Radionics Ltd	390-0464 390-1805 390-0284 390-0278 390-0183 390-2094 390-2252 499-245 546-9656
Safety switch	Magnetic Non-Contact Safety Switch	Radionics Ltd	797-4860
USB microscope	USB microscope AM4113TL	Radionics Ltd	888-2897
Spacer block	Ertacetal C, black	Custom machined	Custom part (plate_spacer.pdf)
Insulating plate	Ertacetal C, black	Custom machined	Custom part (insulating_plate.pdf)
Aluminium plate	Aluminium 1050	Custom machined	Custom part (print_plate.pdf)

contact area between the leadscrew and the carriage nut. For the Z slide defining vertical movement of the print head, resolution is a much greater consideration and high translation speeds are not required. Thus, a low lead is desirable here allowing for the print head to be moved in tiny increments of several microns or less. Here, a Velmex E25 single start leadscrew was chosen, with a lead and pitch of 0.025" (0.635 mm). These leadscrews were mounted within Velmex XSlide assemblies with integrated limit switches. Arcus NEMA 23 stepper motors with a step angle of 1.8° (200 steps per rotation) were mounted to each of the XYZ linear slides. A microstep setting of 50 was further applied to each motor to reduce the effective step size and further allow smoother motion. Framing and motion system assembly components are listed in Table 1. Technical drawings for custom motion assembly parts are included in the [supplementary information](#).

2.3. Print head assembly

The print head assembly is comprised of components responsible for 3 primary functions: (1) application of heat to melt the print material, (2) application of pressure to extrude the print material through the nozzle and (3) application of a high voltage for the stabilisation of micro/nano-fibrous jets for MEW. A similar configuration was used to that from a custom MEW in the Hutmacher lab [24], whereby a tube heater is used to heat the syringe barrel and a ring heater is used to heat the nozzle. An exploded view demonstrating the design of the main print head assembly housing the heaters is illustrated in Fig. 3 A, with the inset illustrating the assembled print head. Fig. 3B shows the actual exploded view of the main print head components with the inset again showing the assembled parts. Ketron® PEEK was used for the upper and lower housing components, which is rated for a 250 °C continuously, while the print head mount was fabricated using a Formlabs 3D printer. Nylon bolts were used to attach the upper and lower housing components to eliminate any possible interference with the high voltage

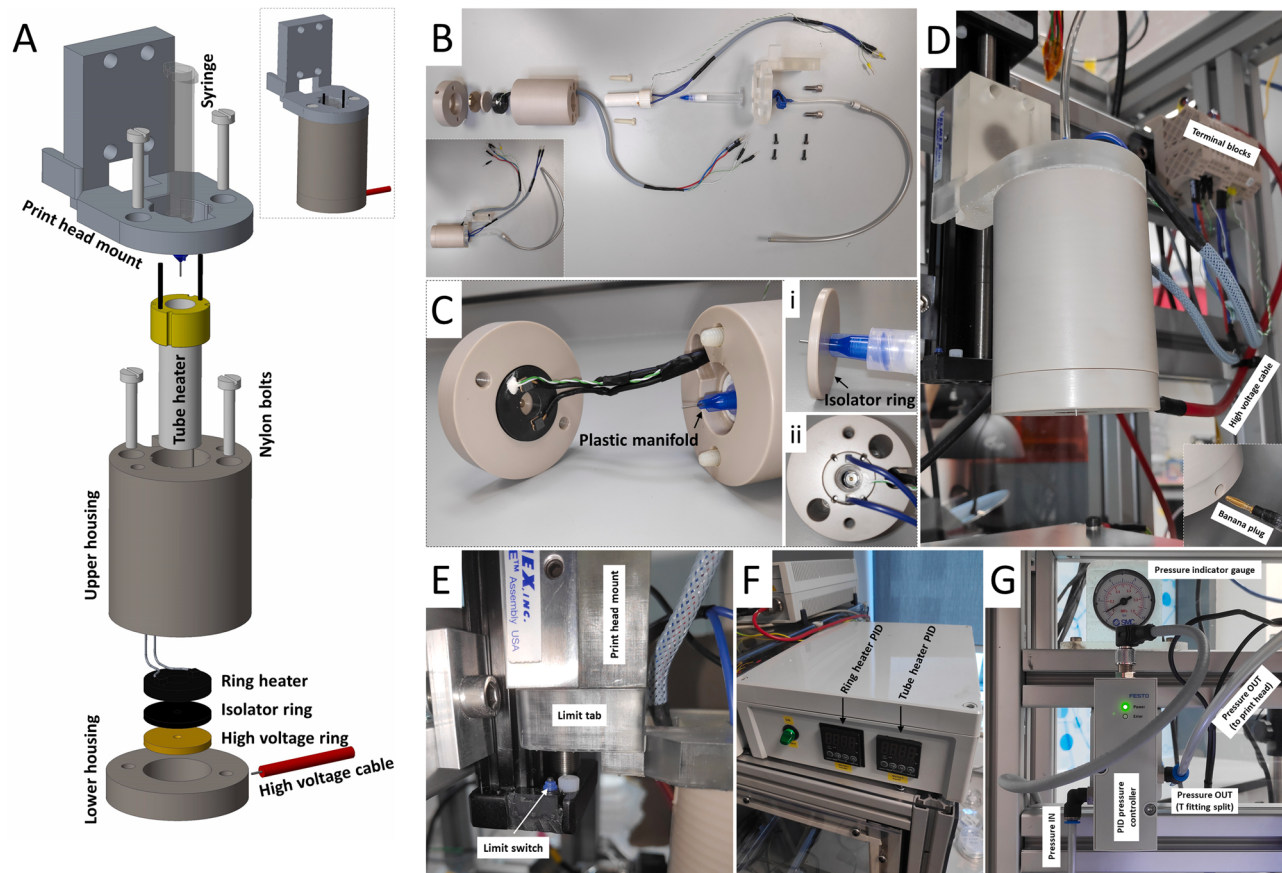


Fig. 3. Print head for MEW printer. **A** CAD design of X-Y stage and print head assembly. **B** Exploded view of print head assembly with detail showing thermocouple attachment to ring heater. **C** Assembled upper and lower print head sections showing placement of heater and wiring. **D** Completed print head mounted to linear slide. **E** Limit tab on print head mount to home slides and accurately define nozzle height while also ensuring the print head cannot collide with the plate. **F** Temperature control unit with a PID controller for each of the two heaters. **G** Set-up for accurate PID control of air pressure for material extrusion. Please see “[Fig. 3. png](#)” in supplementary files for high resolution source image file of figure.

applied to the nozzle. The main obstacle when designing a MEW print head is eliminating any potential interference and electrical arcing between the high voltage applied to the nozzle, and the heaters (or any other electrically conducting components) in the print head. To help mitigate this, an aluminium oxide ceramic tube heater (Rauschert GmbH, Germany) and silicon nitride type HI ceramic ring heater (BACH Resistor Ceramics GmbH, Germany) were used to heat the syringe barrel and nozzle respectively. Nonetheless, there are still metallic components within these heaters and within the wiring and thermocouples, and thus, further measures were taken to physically isolate the nozzle from the heaters. This was done in the form of a PEEK isolator ring designed to fit tightly around the circular plastic manifold at the interface between the nozzle and Luer-Lock connector ([Fig. 3C](#), [Fig. 3C-i](#)). Voltage is applied to a brass ring which fits tightly around a 22 G nozzle/needle and contains a bore in the side to plug in the high voltage lead with a banana plug soldered to the end (Inset, [Fig. 3D](#)). The ring heater, isolator ring and high voltage ring can be seen in a plan view of the assembled print head ([Fig. 3C-ii](#)). A limit tab on the print head mount is designed to contact the limit switch on the end of the linear Z-slide when the nozzle is 0.5 mm from the build plate ([Fig. 3E](#)). This ensures no collisions can occur between the print plate and the print head, and also allows a datum program to be run to calibrate the axes and set the nozzle distance to a known value before printing. A temperature control unit with 2 proportional-integral-derivative (PID) controllers are used to define temperatures of the tube and ring heaters ([Fig. 3F](#)). The internal design and wiring of this unit will be outlined in further detail in the “Wiring and integration of components and safety systems” section below. A PID digital pressure controller mounted to the printer gantry was used to

control air pressure to extrude the print material ([Fig. 3G](#)). A mains air pressure supply of 5 Bar is fed to the inlet, while a T-splitter fitting at the output goes to a 3 ml syringe containing the print material in addition to an analogue pressure gauge. This pressure gauge gives the user a rough indication of the output pressure to visually verify that the pressure is set as desired. The PID unit is controlled digitally via the main control unit to give a precise output pressure, with details of this being outlined further in the “Wiring and integration of components and safety systems” section below. Print head assembly components are listed in [Table 2](#). Technical drawings for custom print head assembly parts are included in the [supplementary information](#).

2.4. Rotating mandrel

A rotating mandrel was built to allow for the fabrication of tubular scaffolds. An exploded view of the design is illustrated in [Fig. 4A](#), with main considerations of the design being a long mandrel for the fabrication of multiple or large scaffolds, and a system by which to easily change mandrel sizes. An offset stepper motor which drives the mandrel via a belt allows the mandrel length to be maximised within the space limitations of the MEW enclosure. The belt is tensioned by sliding the motor and fastening it on the 4 mounting slots. In addition, the system of jaw couplings allows the mandrel to be quickly changed by loosening and tightening a single grub screw on a shaft collar between the bearing mounts at the left hand side of the mandrel in [Fig. 4A](#). A print plate is also mounted on the mandrel chassis at a similar height to the mandrel, allowing space for initial fibre stabilisation before printing. A photograph of the assembled mandrel is shown in [Fig. 4B](#) with another view

Table 2
Components for print head.

Component	Description/ Material	Source	Part number
Print head mount	High Temp Resin (Formlabs)	Custom 3D printed	Custom part (print_head_mount_v3. stl)
Print head - upper	Ketron® PEEK	Custom machined	Custom part (print_head_upper.pdf)
Print head - lower	Ketron® PEEK	Custom machined	Custom part (print_head_lower.pdf)
Tube heater	Ceramic (Aluminum Oxide)	Rauschert GmbH	8786008 XX
Ring heater	Ceramic (silicon nitride type HI)	BACH Resistor Ceramics GmbH	FLR100175
Thermocouple	Type K thermocouple	Radionics Ltd	110-4482
Isolator ring	Ketron® PEEK	Custom machined	Custom part (isolator_ring.pdf)
High voltage ring	Brass	Custom machined	Custom part (brass_hv. pdf)
Bolts	Nylon	Radionics Ltd	527-814
Pressure controller	Proportional pressure regulator	Festo	570967 (VPPX-6 L-L-1- G18-0L10H-S1)
Pressure controller bracket	Bracket for mounting	Festo	542251 (VAME-P1-A)
Pressure controller cable	Power and control cable	Festo	542256 (NEBU-M12W8- K-2-N-LE8)
Pressure controller fittings	Various	Festo	186117 (QSL-G1/8-6) 186158 (QST-G1/8-6)
Syringe barrel	3cc syringe barrel	Nordson EFD	7012072
Syringe piston	White piston SmoothFlow	Nordson EFD	7012166
Nozzle	22G nozzle/ dispensing tip	Nordson EFD	7018260
Pressure adapter hose	Pressure adapter assembly for 3cc barrel	Nordson EFD	7012341
High voltage power supply	20 kV high voltage power supply	Heinzinger	LNC 20000 – 3 pos

clearly showing the drive belt in Fig. 4 C. The mandrel is grounded using a wrap-around copper braid with good electrically conductive contact being maintained with the small grounded aluminium print plate via spring tensioning (Fig. 4D). Fig. 4E shows the mandrel mounted on the same spacer block used for the print plate with the USB microscope being present on the left for process visualisation. A view from the USB microscope of a tubular scaffold being printed is shown in Fig. 4 F. Mandrel assembly components are listed in Table 3. Technical drawings for custom mandrel assembly parts are included in the supplementary information.

2.5. Wiring and integration of components and safety systems

This MEW was designed such that all of the individual components and systems could be controlled via a central unit, thus allowing a great deal of control over printing variables throughout the scaffold fabrication process. Here, we have termed this the “main control unit”, shown in Fig. 5 A, with the front control panel in Fig. 5B. A wiring diagram for the main control unit is included in the supplementary information (mew_2.0_main_wiring.png), along with wiring diagrams for the motor power/control leads (mew_2.0_motor_wiring.png). The main control unit houses a TRIO-P849 (MC508) 8-axis motion controller (Trio Motion Technology Ltd., United Kingdom) (Fig. 5A-1) which is powered via a

24 V power supply (Fig. 5A-4). Four of the axes of this controller are used to control stepper motors (3 motion axes with an addition fourth axis which may be used for a rotating mandrel). In addition, three axes are designated as digital to analogue converter (DAC) outputs, which can be used to send analogue outputs in the range of 0 – 10 V to external equipment via digital signals defined in the motion controller programs. One of these additional axes is used to control the PID pressure controller which has an operating pressure of 0 – 10 Bar. The output pressure of the PID controller is directly proportional to the voltage signal it receives. For example, an output voltage of 0.75 V from the motion controller sets the output pressure of the controller to 0.75 Bar. The other two DAC axes are used to control the high voltage power supply (Heinzinger® LNC 20000 – 3 pos, Germany), with one output controlling voltage (0 – 10 V output from the motion controller corresponds to 0 – 20 kV at the high voltage power supply) and the other controlling current (0 – 10 V from the motion controller corresponds to 0 – 3 mA at the high voltage power supply). The custom connectors used to send these signals are shown in Fig. 5H. Wiring diagrams for auxiliary control leads to control pressure, current and voltage via the main control unit are included in the supplementary information (mew_2.0_aux_wiring.png). Other wires from the PID pressure controller and high voltage power supply are connected to switches on the main control unit panel (Fig. 5B) to enable and disable these devices. The detail inset in Fig. 5 A shows wiring connections between external devices and the main control unit which are contained inside braided sleeves. The motion controller also has a multitude of other input and output terminals available for other uses, including wiring limit switches on the three motion axes to ensure a safe range of motion of the print plate and print head. Here, 24 V from the controller power supply (Fig. 5A-4) is wired to the switches which are wired as normally closed (NC), such that if either the switch is activated via motion at the end of carriage travel on the linear slides, or if a wire break or fault occurs, motion is stopped. Other terminals on the controller are used to wire the amplifier enable (watchdog) relay output to a safety relay Fig. 5A-2. This safety relay is also wired to an emergency stop button on the front panel (Fig. 5B), stopping all motion if pushed. Another input/output terminal on the motion controller is designated as a 0/24 V output which controls a relay to power off/on the PID temperature controllers (relay shown in Fig. 5A-6). This allows the heaters to be controlled via the main control unit also, which is useful for automatically powering off the heaters at the end of a print job. A safety contactor (Fig. 5A-3) is used as a safety device to control mains 230 V A/C power to the high voltage power supply. This contactor is wired such that if the emergency stop button is pushed, or the enclosure door is opened as detected by a proximity switch (Fig. 5 J), power is disconnected from the high voltage power supply. Resetting the emergency stop or closing the door again will restore mains power to the high voltage power supply, however, the output voltage will remain at 0 V until the On/Off switch is pressed again. The motors have a dedicated 24 V power supply (Fig. 5A-5).

Each heater has a PID temperature controller (Fig. 5A-7,9) and solid state relay (Fig. 5A-8,10), with power being provided by a 24 V power supply (Fig. 5A-11). The front panel of the temperature control unit is shown in Fig. 5 C. A wiring diagram for the temperature control unit is included in the supplementary information (mew_2.0_temp_wiring.png). The rear of the main control unit is shown in Fig. 5D, including the mains 230 V supply to the unit, 230 V output from the main control unit to the high voltage power supply, and various power and control cables for devices in the MEW enclosure. An Ethernet connector is used as the programming and control interface between the control unit and the workstation. The high voltage power supply is shown in Fig. 5E, with the control lead going to the main control unit, ground wire going to the print plate, and HV cable going to the brass high voltage ring around the nozzle. The HV cable came supplied with the high voltage power supply (Heinzinger® LNC 20000 – 3 pos, Germany). The custom power/control leads for the motors are shown in Fig. 5 F, with flying power leads at the MDR connector end being connected to the motor power supply in

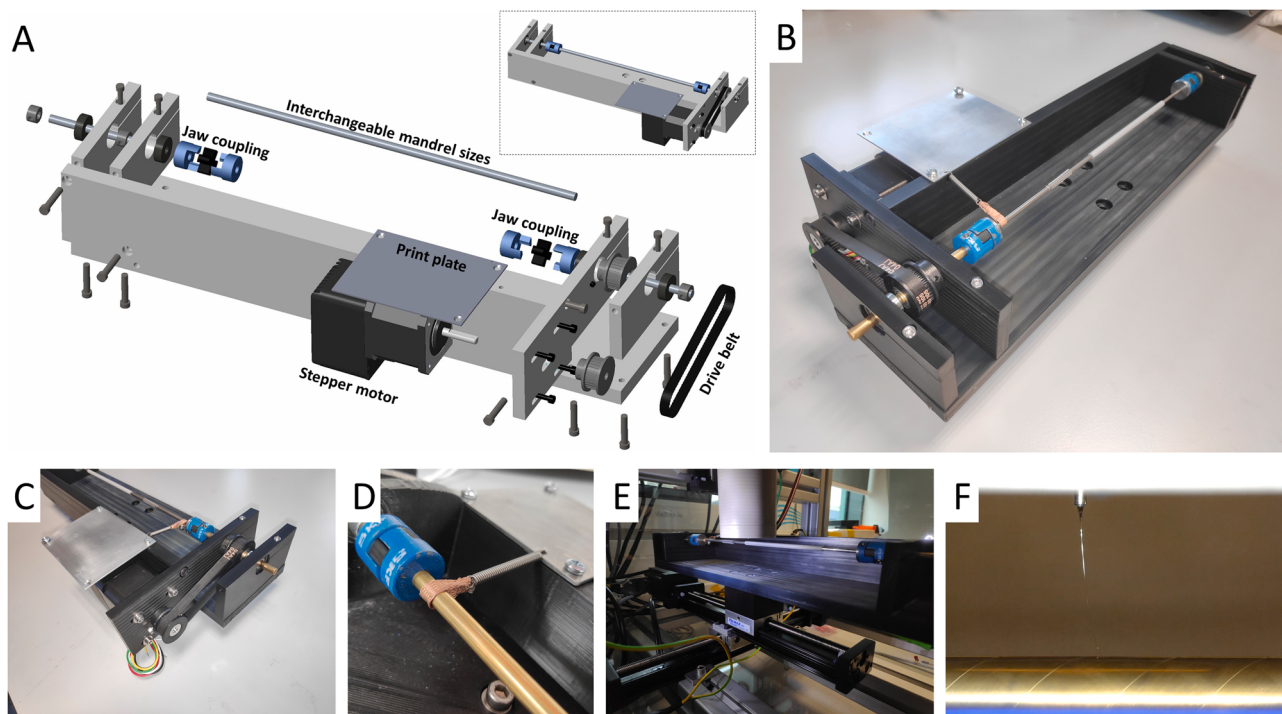


Fig. 4. **A** Exploded view of CAD design of rotating mandrel with inset showing final assembly view. **B** Assembled rotating mandrel. **C** View of drive belt. **D** Mandrel grounding method via a copper braid with good conductive contact being maintained via spring tensioning to a small grounded print plate. **E** Mandrel mounted to the MEW via the same spacer block used to mount the print plate. **F** Image showing stacking of fibres in the process of making a tubular scaffold. Please see “[Fig. 4.png](#)” in supplementary files for high resolution source image file of figure.

[Fig. 5A-5](#). An example of a wired 9-pin D-sub connector is shown in [Fig. 5G](#). These are used for various connections in the MEW, for example, to connect the power/control lead to the motor and to connect the main control unit with the temperature control unit. A series of terminal blocks mounted on a DIN rail on the MEW gantry are used to connect the print head to the temperature control unit ([Fig. 5I](#)). This was done to keep connectors small on the print head side to allow ease of complete assembly and disassembly of the print head. A proximity switch is mounted to the inner side of the enclosure as a safety interlock for the high voltage power supply ([Fig. 5J](#)), as detailed previously.

Components used in the main control unit and temperature control unit are listed in [Table 4](#) and [Table 5](#) respectively. Wiring diagrams are included in the [supplementary information](#).

2.6. Programming and scaffold fabrication

Programming to integrate components is primarily carried out using a form of BASIC programming language called TrioBASIC, which controls the motion/output controller in the main control unit from the “Motion Perfect v4.3” software. Initial set up of all axes is first carried out with the “1_initialise_system.txt” program. This program is set to run automatically on software start-up, after which the “2_zero_stage.txt” program may be run to home all axes and set the print head to a defined height above the collector. Programming for the initial parameters for the auxiliary outputs is done with the “3_set_auxial_variables.txt” program. These programs are included in the [supplementary information](#). Of note here is the “DAC AXIS(X)” command, which is a “digital-to-analog converter” command to convert a numerical value to an output voltage which specifies how an external item of equipment should behave. For example, considering the below series of commands:

$pressure = 1.0$

$DAC\ AXIS(4) = (pressure/10) * 2048$

This sets the pressure of the digital pressure controller to one tenth of its maximum pressure range (10 Bar), which is 1 Bar. Finally, an example annotated program is included in the [supplementary information](#) (4_ke_600um_5mm_high_example.txt). This program includes layer-by-layer voltage and print head height changes to result in a final scaffold height of 5 mm. This is achieved by a series of “MOVE” commands and loops to repeat motion paths a pre-determined number of times until the desired layer height is achieved. Voltage is increased incrementally by 0.0129 kV each layer, and the print head is lifted by 0.0227 mm each layer. At the end of the program, the print head is moved away from the scaffold, voltage and pressure shut off by “DAC AXIS” commands, and the heaters turned off by cutting mains power to the heater power supply in the temperature control unit using the “OP(18,OFF)” command. This command turns off output 18, which in turn sets the output from 24 V to 0 V and de-activates the relay controlling the heater power supply.

In the majority of cases where simple scaffold geometries or those with programmable repeating features are desired, manually programming as in the provided example is relatively quick and straightforward, as the majority of code can be transferred and modified slightly to create similar new programs. Nonetheless, another approach which may be used for more complex scaffold designs is the “CAD2Motion” software package supplied by Trio Motion. This software allows DXF files to be imported and appropriate code to be generated to create more complex motion paths, as with the example for a meniscus shape in “meniscus - CAD2Motion.png” in the [supplementary information](#). DXF files in this case were created using Creo Parametric CAD software, however, there are a host of CAD and other software options to draw DXF files which may be imported. Finally, Trio Motion controllers also have the ability process G-code to control motion if required. In this way, CAD models can be sliced and G-code generated for printing.

Stereomicroscopy and scanning electron microscopy (SEM) was used to image printed structures. For SEM, samples were prepared by mounting on pin stubs with carbon adhesive tabs and coated with gold/palladium for 30–70 s (depending on scaffold size and architecture) at a

Table 3
Components for rotating mandrel.

Component	Description/ Material	Source	Part number
Mandrel base	Ertacetal C, black	Custom machined	Custom part (mandrel_base.pdf)
Mandrel side	Ertacetal C, black	Custom machined	Custom part (mandrel_side_support.pdf)
Mandrel motor mount	Ertacetal C, black	Custom machined	Custom part (mandrel_motor_mount.pdf)
Mandrel bearing mount	Ertacetal C, black	Custom machined	Custom part (mandrel_strut.pdf)
Print plate	Aluminium 1050	Custom machined	Custom part (mandrel_plate.pdf)
Jaw coupling	Coupling to mount various mandrel sizes. X2 needed for each mandrel	Radionics Ltd	837-1057
Mandrel	Round bar of desired size. Brass and stainless steel used. ø = 3.175,5,6 mm	Radionics and Metals4U UK	728-6885 (Radionics) 682-624 (Radionics) 1661-0 (Metals4U) 1676-0 (Metals4U) 1679-0 (Metals4U)
Motor	Integrated NEMA 17 double stack motor + advanced microstep driver	Arcus	ARCUS-DMX-A2-DRV-17-2
Drive belt	RS Pro, Timing Belt, 105 Tooth, 213.36 mm Length X 6 mm Width	Radionics Ltd	778-5060
Drive pulley	RS PRO Timing Belt Pulley, Aluminium, Glass Filled PC 6 mm Belt Width x 2 mm Pitch, 30 Tooth. X2	Radionics Ltd	778-4724
Collar	RS PRO Collar One Piece Screw, Bore 5 mm, OD 10 mm, W 6 mm, Steel. X4	Radionics Ltd	823-6935
Bearing	NSK Deep Groove Ball Bearing - Plain Race Type, 5 mm I.D., 16 mm O.D	Radionics Ltd	408-9754
Other fittings	Stainless steel spring, copper braid	Radionics Ltd	821-419 314-3302

current of 40 mA using a Cressington 208HR sputter coater. Imaging was conducted in a Zeiss ULTRA plus SEM with an accelerating voltage of 5 kV, with the SE2 detector being used for lower magnification imaging to give good topological information and the InLens detector being used for high magnification imaging.

3. Results and discussion

3.1. MEW design

The configuration of the custom MEW printer reported here, with full integration between all of the core components, allows for a high degree of dynamic control over print parameters throughout a print job, allowing for the fabrication of a range of complex architectures. With this configuration, voltage may be regulated throughout the print to fabricate MEW scaffolds with a high thickness [13], and pressure may be controlled throughout the print to fabricate complex architectures with variable fibre diameters [14]. Controlling all components from a central unit also has several practical advantages. For example, all components can be programmed to automatically shut down at the end of a print job, which is advantageous for MEW due to the sometimes long printing times ensuring the user does not need to be present at the end of the print. Indeed, once all physical switches are powered on, the MEW can

also completely be controlled remotely via another computer. This integrated configuration is also advantageous from a safety standpoint, allowing any of the components to easily be linked to the E-stop and safety interlock. A general operating procedure is included in the supplementary information (Operating procedure for trained users.docx).

3.2. Motion system

The MEW system reported here uses mechanical bearing linear slides as the foundation of the motion system, a similar configuration to that used by several different research groups to produce custom MEW printers [12,21,25,26], with stepper motors often being used to drive these slides as is also the case in the present study. The popularity of this configuration lies in the relatively low costs and servicing requirements associated with it, while also being capable of achieving a high degree of positional accuracy and repeatability. Stepper motors are primarily run in an open-loop configuration, relying on pre-defined step counts to define the amount by which to rotate the motor without positional feedback. Nonetheless, these motors are highly capable for MEW applications and in our experience provide exceptional accuracy with no issues even after long, multi-day print jobs. Servo motors have also been used in custom MEW printers [27], and provide additional positional feedback as part of a closed-loop system via the use of encoders to verify and ensure positional accuracy. Various approaches have also been taken for controlling rotating mandrels for the fabrication of tubular scaffolds, with a stepper motor being used in the present work and DC motors being used by others [11,28]. Another good approach which may be taken is to purchase a ready-made motion system, such a multi axis CNC gantry system, and use this as the basis for a custom MEW printer.

Perhaps more important is the design of the system to take into account the differing requirements for the X-Y print plate in comparison to the vertical Z movement of the print head. As detailed previously, the X-Y slides in this work have a larger leadscrew lead value to facilitate the high translation speeds which are required in MEW to print low to sub-micron fibres above their critical translation speed. In contrast, the Z-slide has a much lower leadscrew lead value, prioritising high accuracy and the possibility of extremely low translation distances, which allows for the print head height to be incrementally increased by the thickness of a MEW fibre after each layer of printing if desired. Indeed, depending on the requirements and applications of the user, a motorised Z axis may not even be required [29], however it is advised if there is a requirement to print scaffolds greater than approximately 1 mm in height.

Finally, the configuration of the 3-axis print system also has implications in terms of space restrictions and enclosure size. The MEW printer reported here, as with many other custom systems, has the print plate mounted on an X-Y stage, with the print head moving in the Z direction. This is a relatively simple and intuitive design, however, if a smaller space footprint is required, the print head could be designed to move in 2 – 3 axes, with the print plate moving in either 1 axis or remaining static. In the printer reported here, the print plate has dimensions 21 × 21 cm, with the footprint of the enclosure being 60 × 60 cm to allow for movement of the plate while allowing buffer regions from the framing to electrically isolate the plate and reduce potential pinch hazards. The smaller footprint of the print head vs the print plate means that designing for the print head to move in additional axes would reduce the overall enclosure size required for the same size print plate, at the possible expense of a more complex design.

3.3. Print head configurations

One of the main challenges with building a custom MEW printer is designing the print head such that the print material can be heated while implementing a high voltage (usually several kilovolts, in the range of approximately 1–10 kV depending on nozzle distance) between the nozzle and collector. The high voltage, if applied to the nozzle, has the propensity to arc towards nearby electrically conductive materials, for

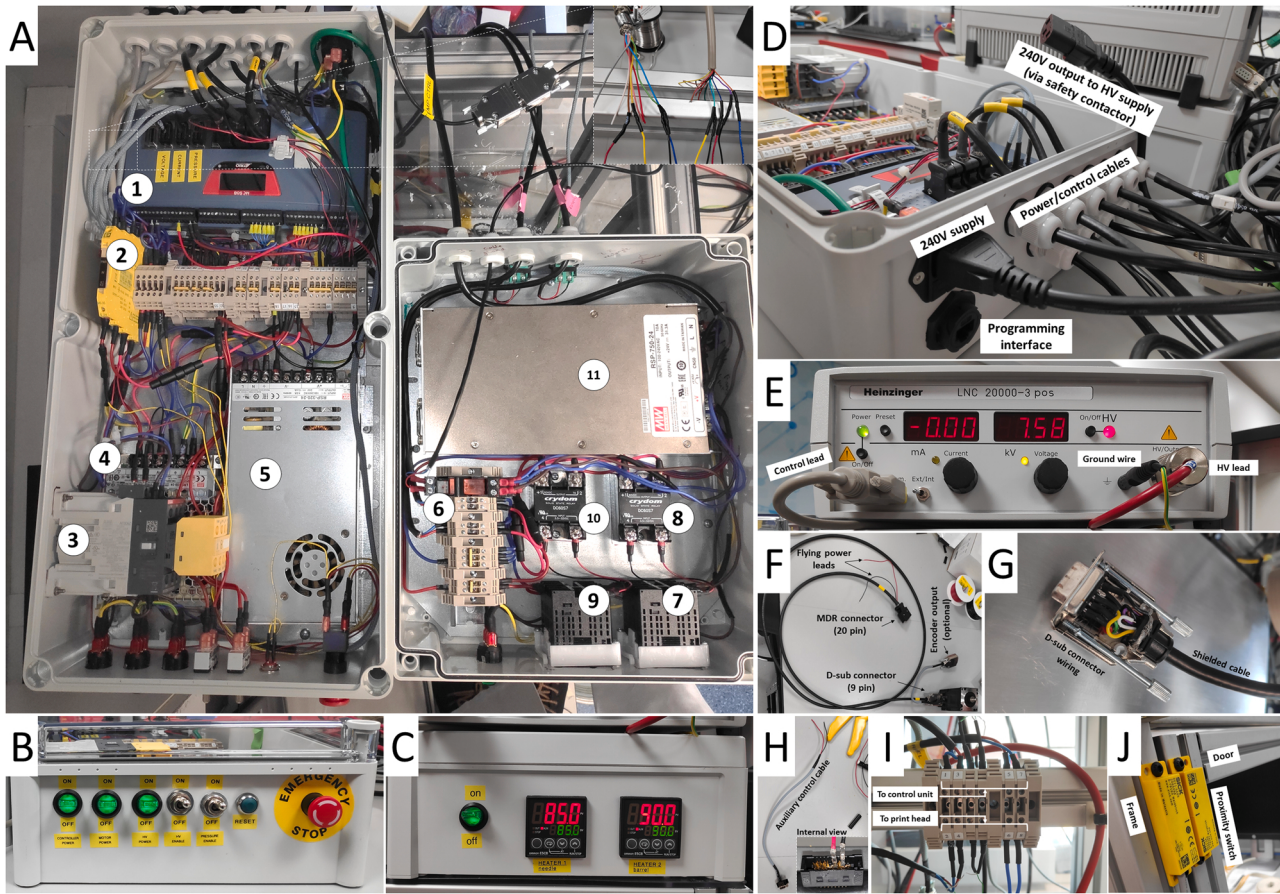


Fig. 5. Wiring and control. **A** Internal wiring of main control unit (left) and temperature control unit (right). Some of the main components include 1. Motion and output controller, 2. safety relay, 3. safety contactor, 4. motion controller power supply, 5. motor power supply, 6. relay to control temperature control unit from main control unit, 7. tube heater PID controller, 8. ring heater PID controller, 9. tube heater solid state relay, 10. ring heater solid state relay, 11. heater power supply. **B** Front panel of main control unit. **C** Front panel of temperature control unit. **D** Output/input cables from main control unit. **E** High voltage power supply with control lead to main control unit. **F** Wiring of motor control leads. **G** Internal wiring of D-sub connectors used for various connections between components. **H** Wiring of auxiliary control cables for communication between the main control unit and the PID pressure controller and high voltage power supply. **I** DIN rail mounted terminal blocks to connect the print head with the main control unit. **J** Proximity switch mounted on the inner door frame as a safety interlock for the high voltage power supply. Please see “Fig. 5.png” in supplementary files for high resolution source image file of figure.

example, the electrical circuitry in the heaters. This is due to the dielectric strength of air, which between flat electrodes has a value of 3 kV/mm [30,31], meaning that above this threshold the insulating properties of air can break down and allow a flow of charge. In all commercially available MEW printers to date, this issue is overcome by applying the high voltage to the collector and grounding the nozzle. In certain cases this may not be desirable however, and may cause issues with arcing, for example, if conducting MEW printing onto a non-planar or irregularly shaped conductive objects or printing on electrically sensitive substrates. In addition, while safety controls are of the utmost importance and should mitigate the possibility in either case, it is easier to accidentally come in contact with residual charge on a large print plate at high voltage in comparison to a nozzle at high voltage in the print head. In this work, we have designed the system such that high voltage is applied to the nozzle with the print plate being grounded, with several measures being taken to mitigate electrical arcing within the print head. Firstly, ceramic heaters have been used, and while these contain embedded electrically conductive materials and several locations with exposed electrical connections, they provide a robust initial barrier to electrical arcing. Secondly, exposed electrical contacts and wires have been insulated as best possible using sheaths and heat shrink tubing. And finally, we implemented a physical barrier in the form of a 2.5 mm thick polyether ether ketone (PEEK) isolator ring which fits tightly around the plastic manifold of the syringe nozzle and sits between the nozzle and

the heaters. The much higher dielectric strength of 24 kV/mm of Ketron PEEK compared to air thus greatly increases the threshold above which arcing may potentially occur. This allows the maximum voltage of 20 kV to be reached in the system without any issues, as has been experimentally verified. Other controls to apply heat to the syringe while overcoming arcing are also possible, such as using a water jacket heating, [1], air heating [17,19] or oil heating [20] approach. Using water however limits the maximum temperature achievable, and in our experience, using air does not provide as stable a temperature and consistent a fibre as using resistive heating elements. We have also designed the present system such that an inverse configuration of high voltage at the print plate and ground at the nozzle is possible if desired. Here, the 210 × 210 mm aluminium print plate sits on a 230 × 230 mm Ertacetal isolator plate with a 10 mm buffer region all around and thickness of 20 mm, thus allowing ample space all around to overcome the potential of arcing to surrounding objects such as the framing. Aluminium was used for the print plate due to its lightweight nature, however, other conductive materials may be used, for example, steel [14,32] or copper [33]. In addition, the use of Ertacetal as a material for the isolator plate is not critical, and other electrically insulating plastics may be used.

In the print head, we have used two heaters, with one heating the syringe barrel and one heating the nozzle, as has also been reported previously in custom built MEW printers [21,34]. This allows the bulk of

Table 4

Components for main control unit. Wiring done as per wiring diagrams in the supplementary information.

Component	Description/Material	Source	Part number
Main controller	Motion Controller - 8 axis Stepper/ servo	Trio Motion Technology Ltd.	TRIO-P849 (MC508)
Controller power supply	Mean Well 108 W Embedded Switch Mode Power Supply, 24 V dc	Radionics Ltd	106-5846 (LRS-100-24)
Motor power supply	Mean Well 321.6 W Embedded Switch Mode Power Supply, 24 V dc	Radionics Ltd	777-2850 (RSP-320-24)
Safety contactor	ABB Jokab AFS Safety Contactor - 25 A, 24 V dc Coil, 3NO	Radionics Ltd	175-3199 (1SBL136082R3022 AFS09Z-30-22-30)
Safety relay	Phoenix Contact 24 V dc Safety Relay - Dual Channel With 1 Safety Contact 1 Auxiliary Contact, PSRmini Range	Radionics Ltd	893-7727 (2904953)
Terminal blocks	RS PRO Din Rail Terminal, 28 → 12 AWG, 2.5 mm ² , 800 V	Radionics Ltd	878-7503
Terminal end bracket	End Bracket	Radionics Ltd	878-7553
Switches	Various (AC switches, DC switches, push button)	Radionics Ltd	419-855 251-9253 (631 H/2) 891-9848
Emergency stop	APEM Panel Mount Emergency Button	Radionics Ltd	219-5813 (A01ES-DM+A0154B-D+A01YL1)
MDR connector	Connector to interface main controller to inputs/outputs of pressure controller and high voltage PSU	Radionics Ltd	163-3285 (10120-6000EL)
Fuse holder	Cooper Bussmann inline fuse holder (alternatively use fused terminal blocks)	Radionics Ltd	849-5594
Connectors/ fittings	Various (RJ45 jack, C14 power plug panel mount, cable glands, D-sub Connectors, nylon sleeves, terminals and connectors)	Radionics Ltd	798-0714 (RDP-5SPFFH-TCU7001) 815-830 (PF0001/63) 822-9644, 787-3820, 170-5425, 170-5419, 135-4167, 135-4166, 135-4169, 135-4168, 534-222, 534-200, 534-446, 186-0303, 680-2366, 239-4212, 452-631
Enclosure	Fibox Polycarbonate Enclosure and base plate	Radionics Ltd	508-2833, 508-3404

material in the barrel to be kept at a lower temperature and reduce thermal degradation, while maintaining a higher temperature in the more constricted manifold and nozzle zone where blockages are more likely to occur with insufficient heating. Even in the case with highly stable materials such as PCL, we have found that keeping the temperature of the barrel approximately 5 °C lower than the nozzle results in a more consistent fibre than equal temperatures or a greater temperature in the barrel heater. If the high voltage will be applied to the print plate

Table 5

Components for temperature control unit.

Component	Description/Material	Source	Part number
PID temperature controller	Omron PID temp controller	Radionics Ltd	772-9376
Relays	Sensata / Crydom solid-state relays	Radionics Ltd	736-0873
Power supply	Mean Well 751 W Embedded Switch Mode Power Supply, 31.3 A, 24 V dc	Radionics Ltd	770-4061
Fittings	Various (terminal blocks, panel connectors, cable glands, switch)	Radionics Ltd	878-7503 455-9742 822-9644 419-855
Relay	24 V dc Coil Non-Latching Relay DPDT	Radionics Ltd	494-0637
Enclosure	Fibox TEMPO ABS Enclosure	Radionics Ltd	104-234

only with the nozzle always being grounded, a simpler and more inexpensive alternative may be to implement a metallic barrel with a standard resistive heating element, as is done in several commercially available MEW printers.

The material of the print head housing is also of importance to ensure stability at the required temperatures. The Ketron® PEEK used here is stable at up to 250 °C continuously, however, if only lower processing temperature materials such as PCL will be used, a more inexpensive material or 3D printed print head housing can be implemented. In this work for example, initial testing of the print head housing design was conducted via a 3D printed version using a commercial 3D printer (Formlabs). For the print head mount, we have used High Temp resin (Formlabs), which was used for its temperature resistance and ease of manufacture via 3D printing. We have experience with this material being stable in this particular use case for extended periods of several years, and ongoing. In certain use cases, for example, if the part will be exposed to UV light for extended periods or if additional loads are placed on the print head, ageing and brittleness of the part may be an issue and other materials may be more appropriate. Alternatively, this mount could also be machined using PEEK, or 3D printed in another material, taking care that its temperature resistance is high enough for desired processing temperatures of the polymer of choice for MEW. The top of the ceramic tube heater does not get as hot as its core temperature, thus, the print head mount does not need excessive temperature resistance.

Finally, the extrusion method used is important both in terms of achieving a consistent flow rate and MEW fibre, and also in terms of limiting degradation of the material. Much of the early research with MEW incorporated syringe pumps to provide flow [10,35,36], however, due to the extremely low flow rates of 5 – 50 µL/hr typically used, getting a consistent flow at this rate is difficult and introduces instabilities into the MEW fibre. The majority of recent work uses pneumatic pressure to extrude material. Air pressure was used in the present work, while nitrogen has also been used [22,37], which as an inert gas may be more desirable to reduce material degradation depending on the material being processed. In the present work, a PID digital pressure regulator was used to give fine control over output pressure while also allowing dynamic pressure changes within the program. Alternatively, while not as precise, favourable results are also possible with manually operated pressure regulators if dynamic pressure changes are not required [17,38].

3.4. Considerations for component integration and MEW safety

In the MEW design reported here, all of the core components are fully integrated and linked to a central “main control unit”. Namely, the motion system, pressure regulator, high voltage power supply and heaters are all linked, allowing a great deal of dynamic control over

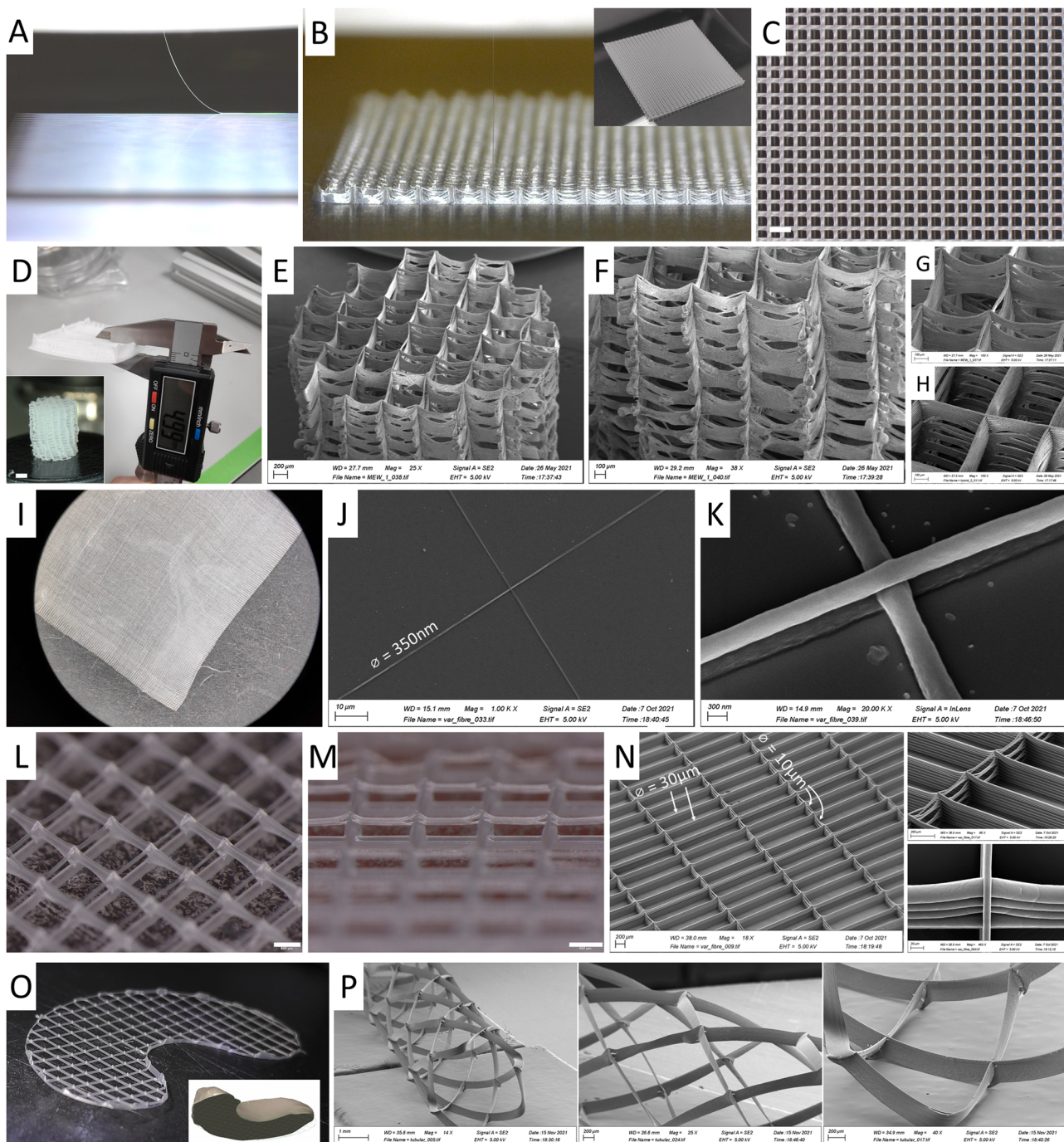


Fig. 6. Scaffolds printed with MEW. **A** Image of fibre mid printing using USB microscope. **B-C** printing of a 1 mm thick scaffold with 0.6 mm pore size (scale = 1 mm). **D** Printing of large volume MEW scaffolds of 5 mm height using via regulating voltage and print head height at each layer, with inset showing a cut cylindrical scaffold of 4 mm diameter (scale = 1 mm). **E** SEM image of 5 mm high scaffold with **F** demonstrating fibre stacking. **G** Top of 5 mm high scaffold showing a well maintained pore structure with **H** showing bottom of 5 mm high scaffold. **I** dense scaffold mesh with fibre diameter of 4 μm and pore size of 0.1 mm. **J-K** Printing of nanometre scale fibres of diameter 350 nm. **L-M** Hybrid scaffold printing with 20 μm MEW fibres stacked on 200 μm FDM fibres, printed in a single print job via pre-programmed pressure control, voltage control and an automated fibre stabilisation sequence between FDM and MEW layers (scale = 500 μm). **N** Printing variable MEW fibre diameters in a single print with 30 μm fibres in one axis and 10 μm fibres fires in the other axis, with automated pressure changes and fibre stabilisation sequences between layers. **O** Printing more complex shapes using DXF files to define scaffold geometry via a scan of a meniscus. **P** Tubular MEW scaffolds printed on the rotating mandrel showing well defined stacking of fibres. Please see “Fig. 6.png” in supplementary files for high resolution source image file of figure.

MEW printing. This also provides additional ease of use benefits, such as automating start up sequences and beginning a print automatically, automatically shutting down all components after a print, and allowing remote control over the MEW via the main software interface from an external computer. It is also possible to build a highly capable MEW printer with discrete components which are not interconnected, or to

design a MEW printer with any level of component integration in between. For example, if large height scaffolds are desired, it is a necessity to have some form of dynamic voltage control to increase voltage as the print head rises throughout the scaffold height. If variable fibre diameters or hybrid FDM/MEW printing is desired, dynamic pressure or flow rate control is advantageous to vary material flow rates. However,

it is worth noting that a certain degree of dynamic fibre diameter control is also possible using only velocity changes to mechanically stretch the fibre, as has previously been reported [14]. With regard to the heaters, there are limited cases where temperature changes may be required throughout the print, and thus in the present work, initial temperatures are defined and only the power to the heaters is controlled from the main control unit via a relay. This allows the heaters to be shut down automatically when a print is complete.

Regardless of the level of complexity of component integration chosen, it is paramount that no effort is spared on implementing effective safety systems. The main concern here is in relation to the high voltages required by MEW. In this work, a magnetic safety switch is mounted to the inner surface of the door and frame, with this being done to eliminate the possibility of overriding the switch should it be mounted on the outer door surface. An emergency stop button is also mounted to the main control unit, with both this and the safety switch being connected to a safety contactor which controls mains electrical power to the high voltage power supply. Also of importance is that the high voltage output does not automatically turn on again if the door is closed or emergency stop button reset, and must be manually switched on again on the high voltage power supply panel. In this work, the emergency stop button (but not the door safety switch) is connected to the motors also, with a similar restart procedure whereby if the emergency stop button is pushed and reset, motion does not automatically re-start, and a reset button must first be pressed on the main control unit. Depending on the requirements of the end user, the magnetic safety switch could also be connected to the motors such that motion is stopped should the door be opened.

3.5. Printing capabilities

Here, scaffolds are primarily fabricated using TrioBASIC programs as outlined in the materials and methods section above. Fig. 6A-B illustrates views from the USB microscope showing scaffolds being fabricated, while Fig. 6 C shows a stereomicroscope image of a typical MEW scaffold. The capability to fabricate large volume scaffolds is shown in Fig. 6D, where a 5 mm high scaffold is shown, with the inset showing a 4 mm diameter cut from one of these scaffolds. The top and sides of this scaffold is shown in Fig. 6E-F, demonstrating the precise stacking of fibres. The pore structure of the top of the scaffold is shown in Fig. 6 G, demonstrating that good control over fibre placement was maintained right to the end of the print job at 5 mm high. This is important to verify for large scaffolds, and is not trivial to achieve compared to the bottom of a MEW scaffold where good control over fibre placement is more straightforward to control in the initial print phase (Fig. 6H). The capability to produce smaller diameter fibres was also verified, with a dense 4 μm fibre diameter fibrous scaffold shown in Fig. 6I, and nanofiber printing down to 350 nm being shown in Fig. 6J-K. The latter scaffolds were fabricated using a combination of low pressures and high translation speeds to draw out small diameter fibres. The ability to conduct FDM printing and fabricate hybrid scaffolds was also demonstrated (Fig. 6L-M), where 20 μm diameter MEW fibres were stacked on 200 μm diameter FDM fibres. This was done in a single print job with pre-programmed and automated powering on of high voltage and fibre stabilisation sequences before depositing MEW fibres. The ability to define variable fibre diameters via pressure changes was also shown (Fig. 6 N), with 30 μm fibres being deposited in one orientation and 10 μm in another at a 90° offset. The capability to print more complex shapes is shown in Fig. 6 O for the printing of a meniscus shape scaffold. Finally, the ability to control the stacking of fibres to create a well-defined tubular scaffold architecture is demonstrated in Fig. 6 P.

4. Conclusions

MEW is a powerful additive manufacturing technology which has abundant potential for the fabrication of complex, micrometric

resolution scaffolds for a range of applications in tissue engineering and beyond. Here, we have outlined the design and build of a custom MEW printer with advanced fabrication and automation capabilities. We have also discussed the relevance of the various systems used in a MEW printer, and described the various other options and approaches which may be taken depending on the specific requirements of the end user. This work aims to make MEW technology more accessible by firstly informing others interested in developing similar custom devices, and additionally, by providing an insight into the inner workings of MEW technology for potential and existing practitioners in this emerging field of additive manufacturing research.

CRediT authorship contribution statement

Barceló Xavier: Validation, Methodology, Investigation. **Federici Angelica S:** Validation, Methodology, Investigation. **Hoey David A:** Writing – review & editing, Resources, Conceptualization. **Eichholz Kian:** Writing – review & editing, Writing – original draft, Visualization, Validation, Software, Methodology, Investigation, Formal analysis, Data curation, Conceptualization. **Gonçalves Inês:** Validation, Methodology, Investigation. **Kelly Daniel J:** Writing – review & editing, Supervision, Resources, Project administration, Methodology, Funding acquisition, Formal analysis, Conceptualization.

Declaration of Competing Interest

The authors declare the following financial interests/personal relationships which may be considered as potential competing interests: Daniel Kelly reports financial support was provided by Johnson & Johnson Services Inc.

Data Availability

Further data is included in supplementary information.

Acknowledgements

This publication was developed with the financial support of Science Foundation Ireland (SFI) under grant number 12/RC/2278 and 17/SP/4721. This research is co-funded by the European Regional Development Fund and SFI under Ireland's European Structural and Investment Fund. This research has been co-funded by Johnson & Johnson 3D Printing Innovation & Customer Solutions, Johnson & Johnson Services Inc. SEM was carried out at the Advanced Microscopy Laboratory (AML), Trinity College Dublin, Ireland. The AML is an SFI supported imaging and analysis centre, part of the CRANN Institute and affiliated to the AMBER centre.

Author contributions

KFE: design and assembly of custom MEW hardware, design and assembly of custom wiring components, design of electrical circuitry and integration of components, programming, SEM imaging. KFE, DAH, DJK: Conception and design of MEW functionality, manuscript writing. KFE, XB, IG, AF: Assembly of components, wiring of electrical components. KFE, AF: Fabrication of scaffolds.

Appendix A. Supporting information

Supplementary data associated with this article can be found in the online version at doi:10.1016/j.addma.2022.102998.

References

- [1] T.D. Brown, P.D. Dalton, D.W. Hutmacher, Direct writing by way of melt electrospinning, *Adv. Mater.* 23 (47) (2011) 5651.

- [2] D.W. Hutmacher, P.D. Dalton, Melt electrospinning, *Chem. Asian J.* 6 (1) (2011) 44–56.
- [3] Dalton, P.D., Melt electrowriting with additive manufacturing principles. Current Opinion in.
- [4] T.D. Brown, P.D. Dalton, D.W. Hutmacher, Melt electrospinning today: an opportune time for an emerging polymer process, *Prog. Polym. Sci.* (2016).
- [5] A. Nadernezhad, et al., Melt electrowriting of isomalt for high-resolution templating of embedded microchannels, *Adv. Mater. Technol.* 6 (8) (2021), 2100221.
- [6] F. Kotz, et al., Fabrication of arbitrary three-dimensional suspended hollow microstructures in transparent fused silica glass, *Nat. Commun.* 10 (1) (2019) 1439.
- [7] P.D. Dalton, et al., Patterned melt electrospun substrates for tissue engineering, *Biomed. Mater.* 3 (3) (2008), 034109.
- [8] M.W. Felix, et al., Printomics: the high-throughput analysis of printing parameters applied to melt electrowriting, *Biofabrication* (2019).
- [9] P. Miesczanek, et al., Convergence of machine vision and melt electrowriting, *Adv. Mater.* 33 (29) (2021), 2100519.
- [10] T.D. Brown, et al., Design and fabrication of tubular scaffolds via direct writing in a melt electrospinning mode, *Biointerphases* 7 (1–4) (2012) 1–16.
- [11] E. McColl, et al., Design and fabrication of melt electrowritten tubes using intuitive software, *Mater. Des.* 155 (2018) 46–58.
- [12] G. Hochleitner, et al., Additive manufacturing of scaffolds with sub-micron filaments via melt electrospinning writing, *Biofabrication* 7 (2015) 3.
- [13] F.M. Wunner, et al., Melt electrospinning writing of highly ordered large volume scaffold architectures, *Adv. Mater.* 0 (0) (2018), 1706570.
- [14] A. Hrynevich, et al., Dimension-based design of melt electrowritten scaffolds. *Small* 0 (0) (2018), 1800232.
- [15] F.M. Wunner, et al., Design and development of a three-dimensional printing high-throughput melt electrowriting technology platform, *3D Print. Addit. Manuf.* (2018).
- [16] M. Castilho, et al., Hydrogel-based bioinks for cell electrowriting of well-organized living structures with micrometer-scale resolution, *Biomacromolecules* 22 (2) (2021) 855–866.
- [17] K.F. Eichholz, D.A. Hoey, Mediating human stem cell behaviour via defined fibrous architectures by melt electrospinning writing, *Acta Biomater.* 75 (2018) 140–151.
- [18] P. Miesczanek, et al., Automated melt electrowriting platform with real-time process monitoring, *HardwareX* (2021), e00246.
- [19] Tourlomousis, F., et al., Towards resolution enhancement and process repeatability with a melt electrospinning writing process: design and protocol considerations. Proceedings of the ASME 2016 International Manufacturing Science and Engineering Conference, 2016.
- [20] J. He, P. Xia, D. Li, Development of melt electrohydrodynamic 3D printing for complex microscale poly (epsilon-caprolactone) scaffolds, *Biofabrication* 8 (3) (2016), 035008.
- [21] F.M. Wunner, et al., Melt Electrospinning Writing of Three-dimensional Poly (epsilon-caprolactone) Scaffolds with controllable morphologies for tissue engineering applications, *J. Vis. Exp.* (130) (2017).
- [22] J.C. Kade, P.D. Dalton, Polymers for Melt Electrowriting, *Adv. Healthc. Mater.* 10 (1) (2021), 2001232.
- [23] T.M. Robinson, D.W. Hutmacher, P.D. Dalton, The next frontier in melt electrospinning: taming the jet, *Adv. Funct. Mater.* 29 (44) (2019), 1904664.
- [24] Wunner, F.M., Design and development of an additive manufacturing technology platform for melt electrospinning writing: A systems engineering approach. 2018.
- [25] N. Abbasi, et al., Calcium phosphate stability on melt electrowritten PCL scaffolds, *J. Sci.: Adv. Mater. Devices* 5 (1) (2020) 30–39.
- [26] M. Castilho, et al., Mechanical behavior of a soft hydrogel reinforced with three-dimensional printed microfiber scaffolds, *Sci. Rep.* 8 (1) (2018) 1245.
- [27] R. McMaster, et al., Tailored melt electrowritten scaffolds for the generation of sheet-like tissue constructs from multicellular spheroids, *Adv. Healthc. Mater.* 8 (7) (2019), 1801326.
- [28] T. Jungst, et al., Melt electrospinning onto cylinders: effects of rotational velocity and collector diameter on morphology of tubular structures, *Polym. Int.* 64 (9) (2015) 1086–1095.
- [29] G. Hochleitner, et al., Fibre pulsing during melt electrospinning writing, *BioNanoMaterials* (2016).
- [30] Berger, L.I. Dielectric strength of insulating materials.
- [31] Tan, D., H. Li, D. Xiao. Analysis on Failure causes of bushing used in 40.5kV metal enclosed air insulation switchgear, in: 2014 China International Conference on Electricity Distribution (CICED). 2014.
- [32] U. Saha, et al., A deeper insight into the influence of the electric field strength when melt-electrowriting on non-planar surfaces, *Macromol. Mater. Eng.* 306 (12) (2021), 2100496.
- [33] H. Ding, et al., A fundamental study of charge effects on melt electrowritten polymer fibers, *Mater. Des.* 178 (2019), 107857.
- [34] M. de Ruijter, et al., Out-of-plane 3D-printed microfibers improve the shear properties of hydrogel composites, *Small* (2017), 1702773–1702.
- [35] T.D. Brown, P.D. Dalton, D.W. Hutmacher, Direct writing by way of melt electrospinning, *Adv. Mater.* 23 (47) (2011) 5651–5657.
- [36] B.L. Farrugia, B.T. Upton, Z. Hutmacher, D.W. Dalton, P.D. Dargaville TR., Dermal fibroblast infiltration of poly(ε-caprolactone) scaffolds fabricated by melt electrospinning in a direct writing mode, *Biofabrication* 5 (2013) 2.
- [37] C. Mota, et al., Melt electrospinning writing of three-dimensional star poly (ε-caprolactone) scaffolds, *Polym. Int.* 62 (6) (2013) 893–900.
- [38] K.F. Eichholz, et al., Development of a new bone-mimetic surface treatment platform: nanoneedle hydroxyapatite (nnHA) Coating, *Adv. Healthc. Mater.* 9 (24) (2020), 2001102.